

## Title: Experimental study of the $^3\text{He}$ and neutron spin structure at low $Q^2$ using a polarized $^3\text{He}$ target

---

**Nguyen Ton\***<sup>†</sup>

*University of Virginia*

*E-mail:* [ton@jlab.org](mailto:ton@jlab.org)

The Jefferson Lab (JLab) Hall A E97110 experiment performed a precise measurement of the neutron spin structure functions at low  $Q^2$  by using a polarized  $^3\text{He}$  target as an effective polarized neutron target. The goals of the experiment are to make a bench-mark test of Chiral Perturbation Theory calculations and to check the Gerasimov-Drell-Hearn (GDH) sum rule by extrapolating the integral to the real photon point. The data were taken in two experimental run periods. The first period covered the lowest  $Q^2$  points but with a defective equipment which complicates the data analysis. The second period covered higher  $Q^2$  point, with a properly working equipment. Preliminary results from second period will be discussed. The spin structure functions  $g_1$  and  $g_2$ , and the spin-dependent partial cross section  $\sigma_{TT}$  of  $^3\text{He}$  and neutron will be discussed.

*The 9th International workshop on Chiral Dynamics  
17-21 September 2018  
Durham, NC, USA*

---

\*Speaker.

<sup>†</sup>On behalf of the small angle GDH collaboration

## 1. Physics motivation

In scattering experiments off a nuclear or nucleon target, the GDH (Gerasimov-Drell-Hearn)[1] sum rule for real photon ( $Q^2=0$  where  $Q^2$  is the momentum transfer) relates the static properties of the target particle's ground state to dynamic properties of all its excited states. The expression for a spin-1/2 target is:

$$I(Q^2 = 0) = \int_{\text{thr}}^{\infty} (\sigma_{1/2} - \sigma_{3/2}) \frac{d\nu}{\nu} = -2\pi^2 \alpha \frac{\kappa^2}{M^2}, \quad (1.1)$$

where  $\sigma_{1/2}$  and  $\sigma_{3/2}$  are the photo absorption cross sections and the subscripts are the total nucleon photon helicity,  $\nu$  is the laboratory photon energy,  $\kappa$  is the anomalous magnetic moment of the target and  $M$  is its mass.

On the other side, Bjorken sum rule holds in the Bjorken limit ( $Q^2 \rightarrow \infty$ )[2]. It relates structure functions of the proton and neutron to the nucleon axial coupling constant in weak decay. These two sum rules belong to domains where calculations are achievable but use different degrees of freedom (hadronic degrees of freedom at low  $Q^2$  versus partonic degrees of freedom at large  $Q^2$ ). Meanwhile, different methods have been used to connect the two sum rules at finite  $Q^2$  values: Chiral Perturbation Theory is used to expand the GDH sum rule while the Operator Product Expansion is used to expand the Bjorken sum rule.

The first approach to generalized the sum rule was proposed by X. Ji and J. Osborne [3] using virtual photon Compton amplitude. While the Compton amplitude cannot be measured directly, it can be accessed indirectly by using dispersion relation:

$$\bar{\Gamma}_1(Q^2) \equiv \int_0^{x_0} g_1(x, Q^2) dx = \frac{Q^2}{8} \bar{S}_1(0, Q^2) \quad (1.2)$$

where the bar indicates exclusion of the elastic contribution. This sum rule can be used to benchmark the agreement between theoretical methods relevant at a given  $Q^2$  and experimental data.

Improvements in polarized beam and target techniques have made it possible to test these theories in finite  $Q^2$  region. Recently, the availability of experimental results in the low and medium  $Q^2$  regions allow us to test the GDH and related sum rules in the non-perturbative region. Results for the generalized GDH sum rule on neutron is shown in Fig. 1, where the blue triangles are results from JLab experiment E94-010 [4] from pion threshold to  $W = 2$  GeV. The blue data show a smooth transition from partonic degrees of freedom to hadronic degrees of freedom. From the MAID model and  $\chi$ PT calculations, one expects a sharp change in slope happening at  $Q^2 < 0.1$  GeV<sup>2</sup>. It's unclear the discrepancies between data and calculations are due to the  $Q^2$  is not low enough, or the  $\chi$ PT calculations.

Moreover, there are several theoretical predictions in this region and their predictions disagree with each others. Hence, measurement of the neutron spin structure at low  $Q^2$  will provide a benchmark test of  $\chi$ PT and help guide the theoretical progress in the transition region from partonic to hadronic degrees of freedom.

The Jefferson Lab (JLab) Hall A E97110 experiment performed a precise measurement of polarized cross sections at  $0.02 < Q^2 < 0.3$  GeV<sup>2</sup> by using a polarized  ${}^3\text{He}$  target as an effective polarized neutron target. The measured data will allow us to test predictions of Chiral Perturbation Theory at very low  $Q^2$ . Furthermore, the extrapolation to the real photon point ( $Q^2=0$ ) will test the GDH sum rule on neutron.

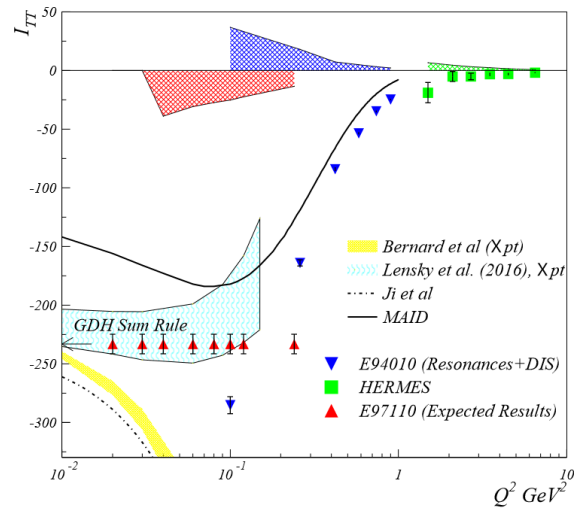


**Figure 1:** Results and expectations for the neutron generalized GDH sum  $I_{TT}(Q^2)$ . Blue triangles are the JLab experiment E94-010 results [4]. Green squares are the HERMES results [5]. Red triangles are the expected results from JLab experiment E97-110. Uncertainty on each data point is statistical only, systematic uncertainties are given by the top band. The solid black line is MAID model calculation. Three  $\chi$ PT predictions at low  $Q^2$ . Ji *et al.* [6](dot line) use HB $\chi$ PT. Bernard *et al.* [7] (yellow band) use HB $\chi$ PT calculations that include  $\Delta$ , where the band is the result of the uncertainties on the parameters of  $\Delta$ . Lensky *et al.* [8] (cyan band) use relativistic B $\chi$ PT. The arrow is the GDH sum at  $Q^2 = 0$ .

## 2. Experimental setup

Experiment E97-110 was carried out in experimental Hall A at JLab. The experiment performed a precise measurement of the neutron spin structure functions at low  $Q^2$  ( $0.02 < Q^2 < 0.3$   $\text{GeV}^2$ ) by using a polarized  ${}^3\text{He}$  target as an effective polarized neutron target. We measured the inclusive reaction  ${}^3\vec{H}e(\vec{e}, e')$  with a longitudinally or transversely polarized  ${}^3\text{He}$ . Eight beam energies  $E$  and two scattering angles  $\theta$  were used for the experiment. The data cover invariant mass  $W = \sqrt{M^2 + 2Mv - Q^2}$  ( $M$  is the nucleon mass) values from the elastic up to  $2.5$   $\text{GeV}^2$  as show in Fig. 2.

Hall A is the largest experimental hall among all halls. The layout of Hall A is shown in Fig. 3. The key elements include the beam line, the polarized  ${}^3\text{He}$  target, a septum magnet, High Resolution Spectrometers (Left and Right HRS) and its detector packages.

The beam polarization was measured at  $75.0 \pm 2.3\%$  [9, 10]. The beam current ranged from 1 to 10  $\mu\text{A}$ . The data acquisition rate was limited to 4 kHz to keep the deadline below 20%.

The  ${}^3\text{He}$  target was polarized by spin-exchange optical pumping (SEOP) [11]. Two sets of Helmholtz coils give  ${}^3\text{He}$  polarization be either parallel or perpendicular to the beam direction. The average in-beam target polarization was  $39.0 \pm 1.6\%$ .

The scattered electron was detected by a RHRS with a lowest scattering angle of  $12.5^\circ$ . A septum magnet was placed in front of HRS so that  $6^\circ$  scattered electron can be detected.

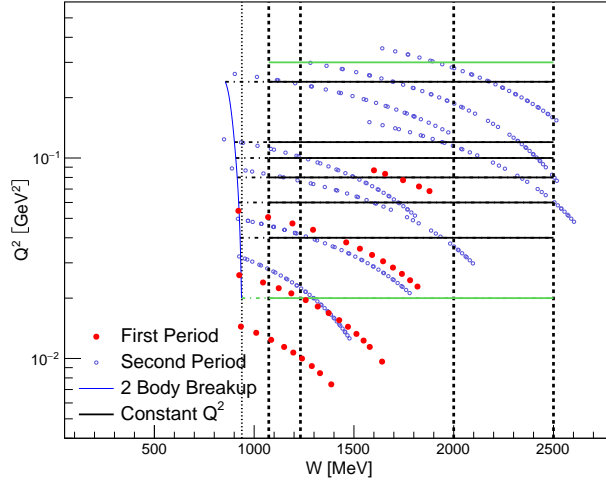


**Figure 2:** Kinematic coverage of experiment E97-110. Horizontal axis is the invariant mass  $W$ . The vertical axis is the  $Q^2$ . The solid horizontal black lines are the constant  $Q^2$ . The value of  $I(Q^2)$  is obtained by integration of the cross section difference over  $W$  at a constant  $Q^2$ .

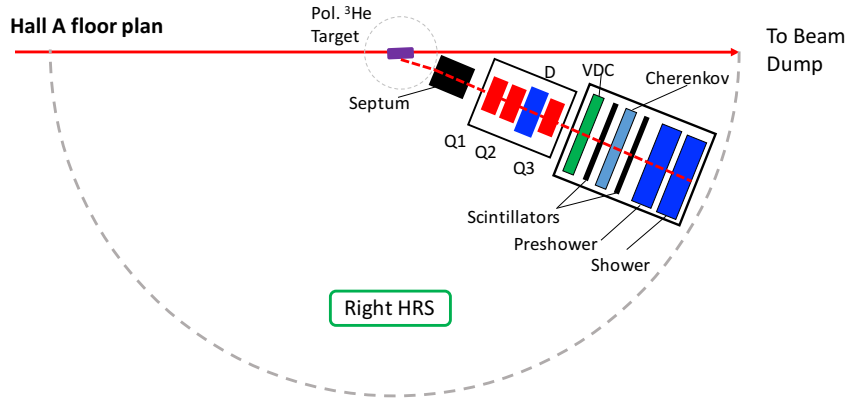


**Figure 3:** Hall A layout. Due to the availability of the septum magnet, only right HRS (RHRS) was used during this period.

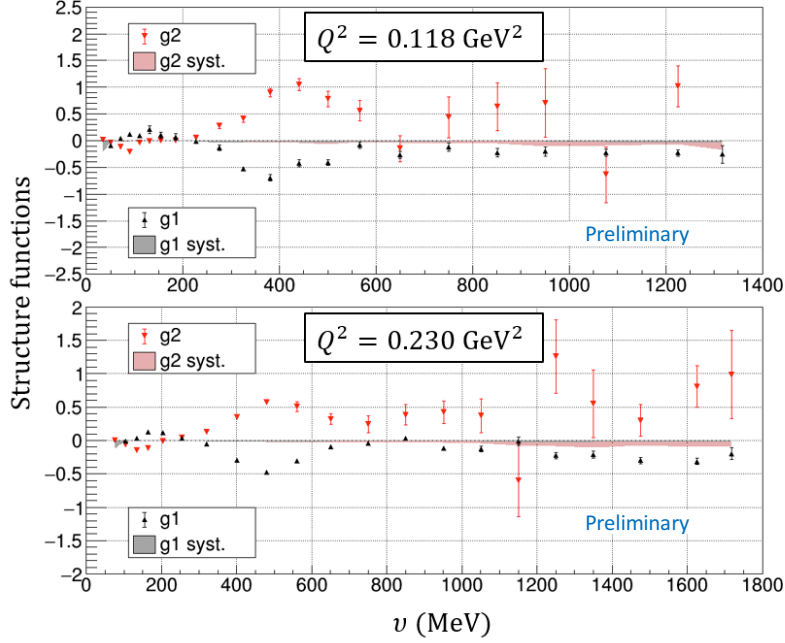
### 3. Preliminary results on $^3\text{He}$ and neutron

The spin dependent structure functions  $g_1$  and  $g_2$  were extracted from the cross section differences:

$$g_1 = \frac{MQ^2 v E}{4\alpha^2} \frac{1}{E' E + E'} \left[ \Delta\sigma_{\parallel} + \tan\left(\frac{\theta}{2}\right) \Delta\sigma_{\perp} \right] \quad (3.1)$$

$$g_2 = \frac{MQ^2v}{8\alpha^2E'(E+E')} \left[ -\Delta\sigma_{\parallel} + \frac{E+E'\cos(\theta)}{E'\sin(\theta)}\Delta\sigma_{\perp} \right] \quad (3.2)$$

where  $\Delta\sigma_{\parallel,\perp} = 2\sigma_0A_{\parallel,\perp}$ . The results for  $g_1$ ,  $g_2$  and for  $\sigma_{TT}$  on  $^3\text{He}$  are shown in Fig. 4 and Fig. 5, respectively. The generalized GDH sum rule of  $^3\text{He}$  is firstly measured for  $Q^2 < 0.1 \text{ GeV}^2$ , and the result shown a turn-over of  $I_{GDH}(Q^2)$  at around  $0.1 \text{ GeV}^2$ . In addition, our data reveal a changing in slope hence suggest the recovery of the GDH sum rule at the real photon point.



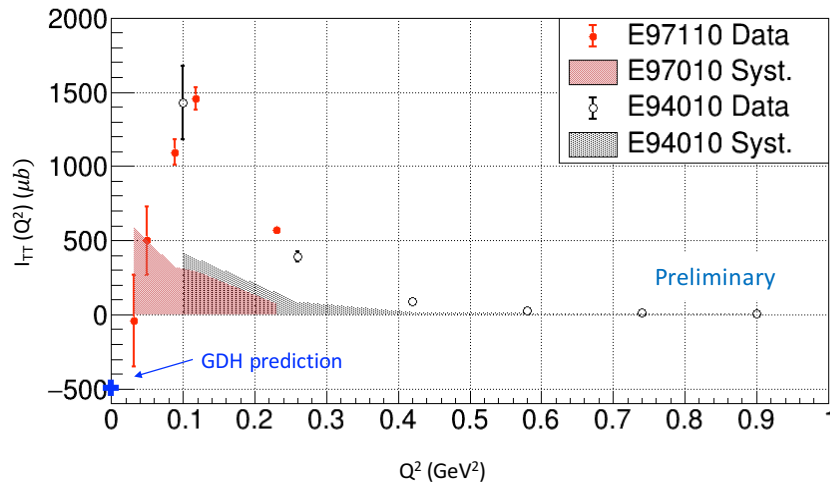
**Figure 4:** Spin dependent structure functions for  $Q^2 = 0.118$  and  $0.230 \text{ GeV}^2$  [12].

Fig. 6 show  $\Gamma_1^n$  for neutron versus  $Q^2$ . The result is compared to theoretical models [7, 8] and previous available data. The error bars represent statistical uncertainty (inner), systematic uncertainty (outer). The range where  $Q^2$  overlap, our data agree with the earlier data extracted either from deuteron or  $^3\text{He}$ . Precision from our measurement is much improved compared to the CLAS data and E94-010 data at larger  $Q^2$ .

Fig. 7 shown  $I_{TT}^n(Q^2)$ . The preliminary results are extracted from the unmeasured high  $W$  part are represented with the open and solid triangles. The error bars represent the statistical uncertainties and the band represent systematic uncertainties. Our results agree well with the earlier data in the overlap region. In addition, the results agree with Bernard *et al.*[7] calculation and disagree with Lensky *et al.*[8] calculation.

Generalized spin polarizabilities offer another test of  $\chi\text{PT}$ . Contrary to first moment, the polarizability integrals have a  $1/v^2$  factor that suppresses the low- $x_{BJ}$  contribution. The generalized forward spin polarizability sum rule and  $LT$ -polarizability sum rule are given as follow:

$$\gamma_0(Q^2) = \frac{16\alpha M^2}{Q^6} \int_0^{x_0} x^2 [g_1(x, Q^2) - \frac{4M^2}{Q^2} x^2 g_2(x, Q^2)] dx \quad (3.3)$$



**Figure 5:** The generalized GDH integrals for  $^3\text{He}$ . The blue point at  $Q^2 = 0$  shows the GDH sum rule for real photons. E94-110 data points are provided by [13]

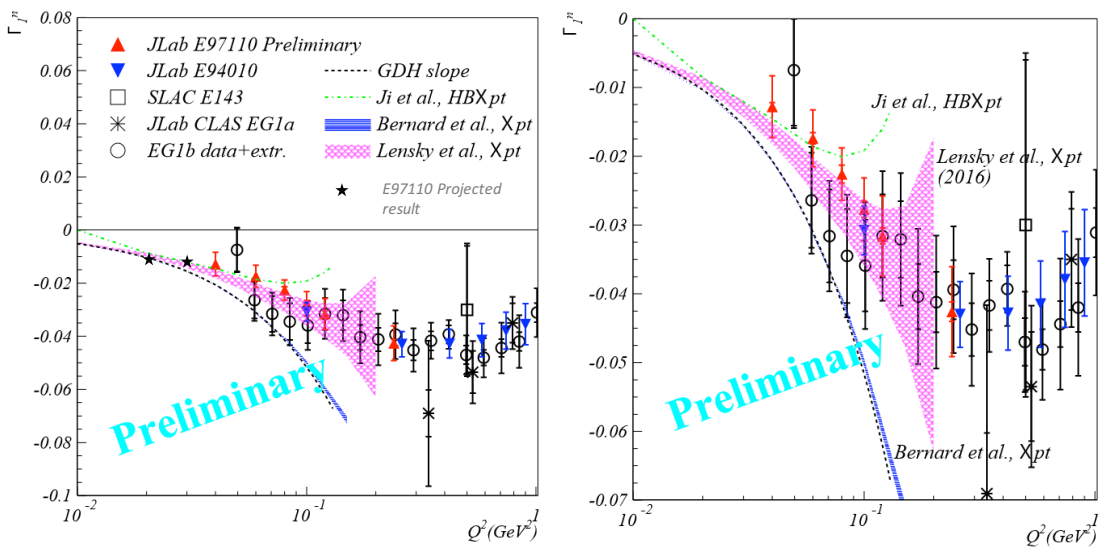


**Figure 6:** The neutron  $\Gamma_1$  versus  $Q^2$ , compared to the world data and models. The right plot is zoomed in of left plot.

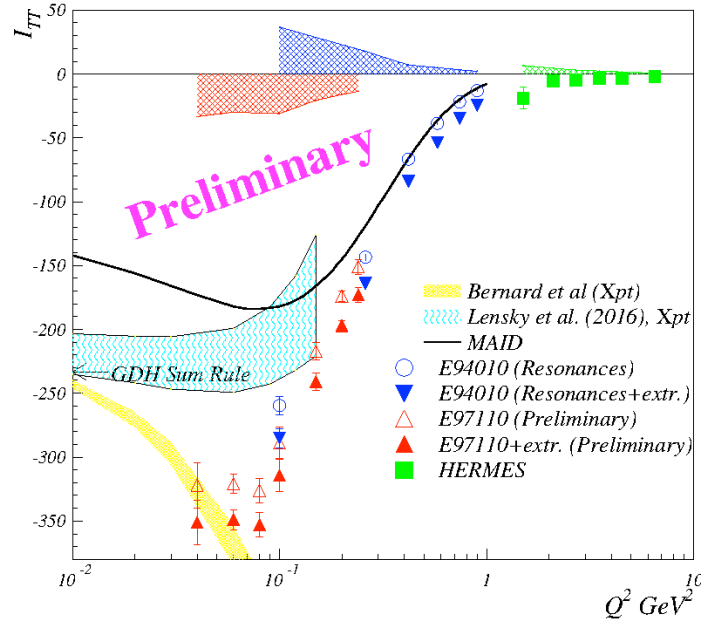


**Figure 7:** The neutron  $I_{TT}(Q^2)$  compared to the world data and models. Red solid (open) triangles are results from this experiment, where the solid is the result with estimated unmeasured high  $W$  contribution and without for open one. Blue data are JLab experiment E94-010 [4].

$$\delta_{LT}(Q^2) = \frac{16\alpha M^2}{Q^6} \int_0^{x_0} x^2 [g_1(x, Q^2) + g_2(x, Q^2)] dx \quad (3.4)$$

$\Delta(1232)$  resonance is suppressed in  $\delta_{LT}$ , making it ideal to test  $\chi$ PT calculations for which the  $\Delta(1232)$  is not included. Fig. 8 shown result of  $\gamma_0^n$  and  $\delta_{LT}^n$  for neutron. The  $\gamma_0^n$  extracted either from  $^3\text{He}$  or deuteron agree well with each other. The MAID model agree with  $\gamma_0^n$  data and so do the  $\chi$ PT results, except Lensky *et al.* calculation.

#### 4. Summary

In summary, spin structure functions  $g_1$ ,  $g_2$  and polarizabilities  $\gamma_0$ ,  $\delta_{LT}$  results were measured at low  $Q^2$ . The data agree with previous measured neutron and deuteron results and with some of  $\chi$ PT calculations. Data from this experiment combined with result obtained on deuteron and future proton results will consolidate our knowledge and calculations from  $\chi$ PT. More data down to  $Q^2 = 0.02 \text{ GeV}^2$  are being analyzed and will check further  $\chi$ PT and status of turn over for  $I_{TT}^n$ .

#### References

- [1] S. B. Gerasimov, *Sov. J. Nucl. Phys.* **2**, 430 (1966) [*Yad. Fiz.* 2, 598 (1965)]; S. D. Drell and A. C. Hearn, *Phys. Rev. Lett.* **16**, 908 (1966); M. Hosoda and K. Yamamoto *Prog. Theor. Phys.* 36 (2), 425 (1966)
- [2] J. D. Bjorken, *Phys. Rev.* **148**, 1467 (1966).

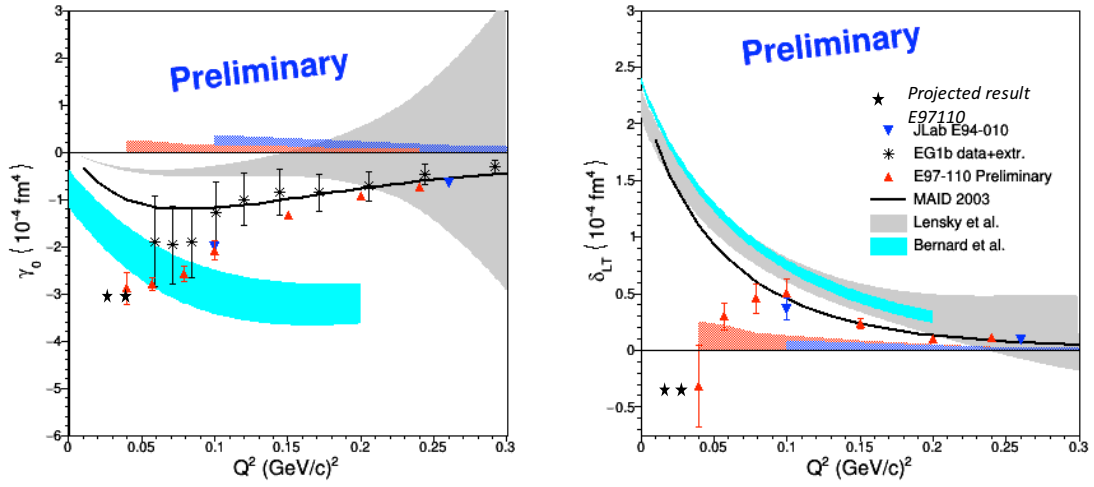


**Figure 8:** The neutron  $\gamma_0$  (left) and  $\delta_{LT}$  (right). Red triangles are results from this experiment. Blue data are JLab experiment E94-010 [4].

- [3] X.-D. Ji and J. Osborne, *J. Phys.* **G27**, 127 (2001).
- [4] M. Amarian *et al.*, *Phys. Rev. Lett.* **89**, 242301 (2002).
- [5] K. Ackerstaff *et al.*, *Phys. Lett.* **B444**, 531 (1998).
- [6] X.-D. Ji, C.-W. Kao and J. Osborne, *Phys. Lett.* **B472**, 1 (2000).
- [7] V. Bernard, E. Epelbaum, H. Krebs and U. G. Meissner, *Phys. Rev. D* **87**, no. 5, 054032 (2013)
- [8] V. Lensky, J. M. Alarcon and V. Pascalutsa, *Phys. Rev. C* **90**, no. 5, 055202 (2014)
- [9] J. Alcorn *et al.*, *Nucl. Instrum. Meth. A* 522, 294 (2004).
- [10] V. Sulkosky *Ph. D. thesis*, Col. of William & Mary (2007).
- [11] <http://hallaweb.jlab.org/experiment/E97-110/>
- [12] C. Peng *Ph. D. thesis*, Duke University (2018).
- [13] Karl Slifer and Ryan Zielinski private communication, 2017.